

MSEC2014-3948

NUMERICAL SIMULATION OF THE AUSTENITIZING PROCESS IN HYPOEUTECTOID FE-C STEELS

Dehao Liu
Tsinghua University
Beijing, China

Gang Wang*
Tsinghua University
Beijing, China
gwang@mail.tsinghua.edu.cn

Zhenguo Nie
Tsinghua University
Beijing, China

Yiming(Kevin) Rong
Tsinghua University
Beijing, China;
Worcester Polytechnic Institute
Worcester, Massachusetts, US

ABSTRACT

For predicting of diffusive phase transformations during the austenitizing process in hypoeutectoid Fe-C steels, a two-dimensional model has been developed. The diffusion equations are solved within each phase (α and γ) using an explicit finite volume technique formulated using a square grid. The discrete α/γ interface is represented by special volume elements α/γ . The result showing the dissolution of ferrite particles in the austenite matrix are presented at different stages of the phase transformation. Specifically, the influence of the microstructure scale and heating rate on the transformation kinetics has been investigated. Final austenitization temperature calculated with this 2D model is compared with predictions of a simpler one dimensional (1D) front-tracking calculation.

INTRODUCTION

During the grinding process of low carbon steels, the temperature of the workpiece rises rapidly and surpasses 727°C , accompanied by austenite formation. The martensite can be found in the surface layer after grinding [1]. In fact, it is arguable that in grinding austenitization may be due to strain-

induced transformation rather than temperature-induced transformation [13]. But temperature-induced transformation is a significant mechanism during the grinding process. Actually, there are some globular crumbs on the surface of the hypoeutectoid Fe-C steel under SEM after grinding, which can't be induced by strain-induced transformation. (see Fig. 1) Therefore, this paper focuses on the influence of temperature-induced transformation during the grinding process.

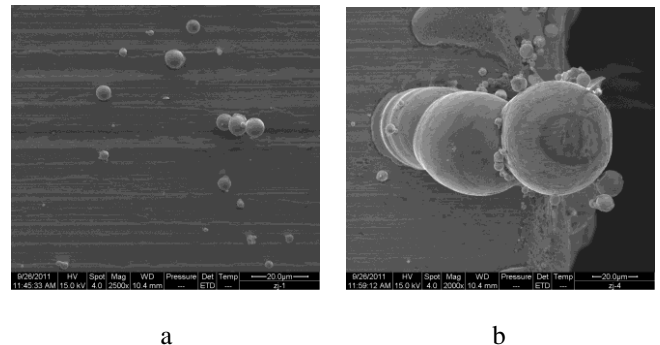


Fig. 1 Globular crumbs of the hypoeutectoid Fe-C steel after grinding

It's important to study the kinetics of austenite formation for grinding process, which has immense value theoretically and practically. Modelling can help us understand austenitizing dynamics better and find some potential microstructural defects during phase transformations of materials. Several models for the prediction of phase transformations in the austenitizing process in hypoeutectoid Fe-C steels have been proposed and progressed remarkably over recent years [5-12]. A two dimension model proposed by Jacot and Rappaz reproduces realistic microstructure with a wide distribution of particle size and morphology, which uses digitized micrographs as a starting microstructure in the form of 2D-images [2-3]. Another way to predict austenitizing process uses Johnson-Mehl-Avrami (JMA) equation to describe non-isothermal solid-state transformations and figure out the activation energy of the phase transformation, which is easier to operate [4].

The austenite formation during heating differs in many ways from those transformations that occur during the cooling of the austenite. The kinetics of austenite decomposition can be described well in terms of the chemical composition and the austenite grain size, but the kinetics of austenite formation is influenced by chemical composition, initial microstructure and the heating rate.

This paper proposes a general two-phase model for the prediction of microstructural evolution in a material which undergoes a diffusive phase transformation α to γ . The diffusion equations in α and γ phases are solved in 2D using an explicit finite volume scheme. The influence of the heating rate and grain size on the kinetics and microstructural evolution of austenite formation were analyzed in the rapid heating of hypoeutectoid carbon steel by using the two dimensional model with square grids. The final austenitization temperature diagram of the steel was also obtained.

MODELING OF THE AUSTENITIZING IN 2D

The kinetics of microstructure formation during austenitization of steels can be predicted by using Fe-C equilibrium phase diagram and some kind of additive principles.

The process of austenitization of steels may be considered to occur in three steps: the pearlite dissolution and then the transformation of proeutectoid ferrite into austenite. The first step occurs above the eutectoid temperature and is governed by the dissolution kinetics of cementite and by the carbon diffusion in the lamellae of the ferrite. It is relatively fast since the diffusion distances are short. Therefore, the first step of

process was not described. The second step occurs within a temperature range which is limited by the eutectoid line and the α/γ transition temperature of pure iron [3]. The third step is the homogenization of the carbon distribution in austenite.

This paper focuses on the transformation of proeutectoid ferrite into austenite and makes the following assumptions:

- The temperature is uniform in the calculation domain. This assumption is justified since the thermal diffusivity is much higher than the solute diffusivity in metals.
- The condition of local equilibrium is applied, so that the carbon concentration at the interfaces can be deduced from the phase diagram for a given temperature modified by the curvature contribution.
- The cementite has dissolved entirely and there are only the ferrite and the austenite in the steels.

Assuming that the α/γ transformation is only governed by solute diffusion, the kinetics can be described by the following diffusion equations:

$$\frac{\partial C_v}{\partial t} = \text{div}[D_v(C_v, T) \text{grad} C_v] \quad (1)$$

$$C_v(x, t = 0) = C_v^*(T_i) \quad (2)$$

$$D_\alpha(T) = 2.0 \times 10^{-6} \exp\left(-\frac{8.41 \times 10^4}{RT}\right) \quad (3)$$

$$D_\gamma(T) = 2.0 \times 10^{-5} \exp\left(-\frac{1.4 \times 10^5}{RT}\right) \quad (4)$$

where t is the time, C_v is the carbon concentration in the phase v (α or γ) and D_v is the associated diffusion coefficient. The symbol $*$ denotes values taken at the α/γ interface and $C_v^*(T_i)$ is the carbon concentration at the initial temperature T_i , which is given by the phase diagram assuming equilibrium. The temperature history of the specimen, $T(t)$, is a given function of time and is considered to be uniform in the calculation domain. This can be justified by the fact that thermal diffusion is much faster than diffusion of solute atoms.

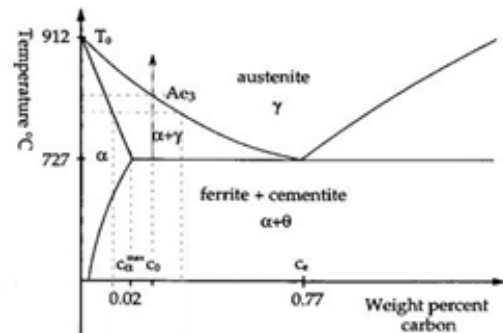


Fig. 2 Fe-C equilibrium phase diagram

Modeling of the two-phase diffusion in two dimensions is much more complex than the 1D equivalent, because the

geometry of the interface must be solved together with the diffusion equation and the normal velocity of the α/γ interface is not so easy to be computed like 1D model. Even the velocity of the α/γ interface can be computed, it will increase the amount of computation markedly and the model will be limited to small size. So this problem can be solve by comparing $C^*(t)$ (the carbon concentration at the α/γ interface at the t moment) with $C_\gamma^*(T(t))$ to judge if the α/γ interface has changed to the γ phase. If $C^*(t)$ exceeds $C_\gamma^*(T(t))$ during heating, then the α/γ interface has changed to the γ phase.

Jacot and Rappaz's 2D model adopts the hexagonal grid, so it becomes difficult to divide meshes and calculate in Cartesian coordinate system. What's more, it's very difficult to apply a hexagonal grid to 3D model. Therefore, the 2D model in this paper adopts a square grid, which is easy to be divided in programs and it can be applied to 3D model without any difficulties. A square volume element (or cell) is attributed to each nodal point and can take three different states: α , γ or the α/γ interface. A layer of interface cells always separates γ from α volume element, which are not allowed to be adjacent (see Fig. 3(b)). The solute concentration in each of these cells is given by C_i , where i is the cell index. The interface cells are characterized by two additional variables: C_α^* and C_γ^* , the solute concentrations at the interface in the α and the γ phases, respectively. Fig. 3(a) shows the space relationship between the central cell i and its neighbors. The arrow represents the flux going from neighbor 1 to the central cell i .

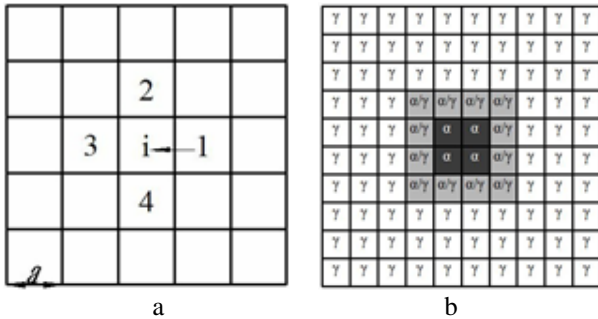


Fig. 3 (a) The space relationship between the central cell i and its neighbors (b) The layer of the α/γ interface cells which separate the α and γ domains

The solute diffusion between the cells is described using an explicit finite volume approach. A mass balance is achieved for each cell i according to the concentration of the four neighboring cells:

$$S \frac{\Delta C_i}{\Delta t} = \sum_{k=1}^4 a J_{ki} \quad (5)$$

with

$$S = a^2 \quad (6)$$

where a is the grid parameter of the square network of cells, S and a are the surface and the edge length of the cells, Δt is the time step, ΔC_i is the variation of carbon concentration in cell i and J_{ki} is the flux of solute atoms from the k -th neighboring cell to the central cell i ($k = 1,2,3,4$). This solute flux is calculated according to the state of the neighboring cells.

(a) The cells k and i belong to the same phase v (α or γ),

$$J_{ki} = D_v(T) \frac{C_k - C_i}{a} \quad (7)$$

(b) The cell i belongs to phase v while cell k belongs to the interface:

$$J_{ki} = D_v(T) \frac{C_v^* - C_i}{a} \quad (8)$$

(c) Both cells belong to the interface:

$$J_{ki} = 0 \quad (9)$$

As the precise relation between diffusion coefficient D_v and carbon concentration C_v is not clear and the influence of C_v is small, it is assumed that D_v is independent of C_v . In order to avoid border effects, periodic boundary conditions are applied to the cells located near the edges. The time step, Δt , is given by the stability criterion of the explicit scheme: it is calculated for the maximum tabulated value of the diffusion coefficient, D_{max} , and is given by:

$$\Delta t < \frac{a^2}{4D_{max}} \quad (10)$$

At each time step, the new carbon concentration of the interface cells is converted into a new phase fraction by comparing $C^*(t)$ with $C_\gamma^*(T(t))$. If $C^*(t)$ exceeds $C_\gamma^*(T(t))$ during heating, the interface cell is attributed to γ . All the α neighbor cells which are adjacent to this cell are changed to interface cells so that α and γ cells are never adjacent.

NUMERICAL SIMULATION RESULTS AND 1D VALIDATION

The 2D model was first applied to a 1D problem in order to compare the results computed by using the Jacot and Rappaz's front-tracking 1D model [2]. A rectangular domain was initially subdivided into two zones (ferrite and austenite) according to a vertical planar interface. Taking the start of the austenitization process at the eutectoid temperature and assuming equilibrium, the initial carbon concentration was set to 0.77 wt% in the austenite and to 0.02 wt% in the ferrite. The initial volumetric phase fraction of ferrite was determined from the nominal composition of the alloy (0.40 wt%) using the lever

rule. The temperature of the domain was then increased at a constant rate of $1^\circ\text{C}/\text{s}$. Assuming local equilibrium at the α/γ interface, the thermal history and the phase diagram directly give the carbon concentration $C_\alpha^*(t)$ and $C_\gamma^*(t)$ of the interfacial cells. Fig. 4(a) shows the change of phase in the domain at four different times together with the 4×50 square grid used for the computations. The vertical green lines are the interface lines in the region. As can be seen, the interface remains stable and planar during the entire transformation process. Concentration profiles are compared with profiles obtained with the 1D model in Fig. 4(b) at different moments (Heating rate $1^\circ\text{C}/\text{s}$, nominal carbon concentration of the alloy 0.40 wt%, grain size 25 μm).

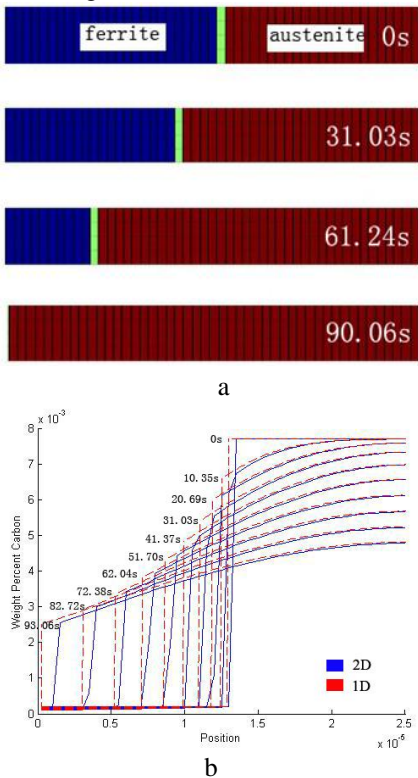


Fig. 4 (a) Changes of phase predicted in the 2D model (b) Concentration Comparison. (Grain size: 25 μm)

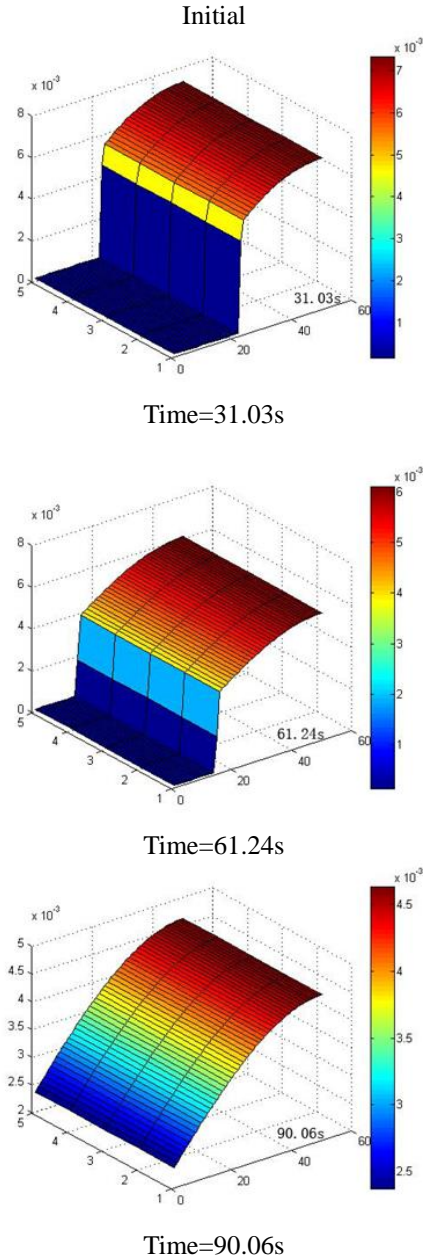
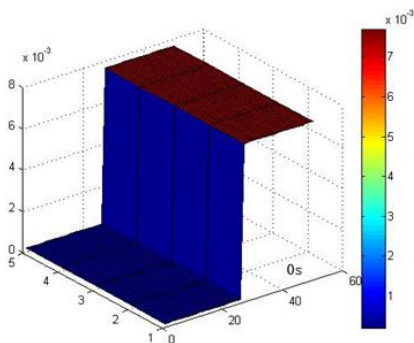


Fig.5 Carbon concentration fields of the 2D model (Grain size: 25 μm)

As expected, the agreement is excellent. The concentration difference in the interface reduces gradually (see Fig. 5). The only difference that can be observed is for the concentration jump at the interface. It is spread over one layer of the mesh in the 2D model, whereas it is a sharp transition in the case of the front-tracking 1D model. It can be concluded that the 2D model correctly predicts the kinetics of the phase transformation and does not introduce interface instabilities in this particular case. Moreover, the numerical diffusion at the interface is limited to one layer thickness.

In order to verify 2D model, Comparisons of final austenitization temperatures in 1D model's corresponding results under different conditions are finished (see Fig. 6). The temperature corresponds to different grain sizes and heating rates. It's obvious that the variation trend of the final austenitization temperature is similar between two models. However, the final austenitization temperature of 2D model is little higher than 1D model's because their microstructure is different and the grids of 2D model are not so dense like 1D model's nodes. So it may take more time for the 2D model to complete the austenitization. As the heating rate or grain size increases, the difference between two models' final austenitization temperature decrease.

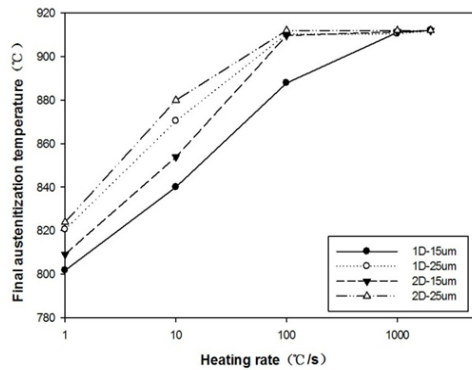


Fig.6 Final austenitization temperature, Fe-0.40 wt% C steel

Then the experiment of fast heated austenitization is carried out using thermal dilatometer DIL805A. The specimen is manufactured into a cylinder with dimension of $\Phi 4 \times 10$ mm. The heating rates are 0.01°C/s, 0.1°C/s, 1°C/s, 10°C/s, 30°C/s, 50°C/s, 100°C/s respectively. The samples are heated from 20°C to 950°C at different heat rates.

Normalized 45 steel is used as the experimental material, and its grain size is 25um from metallography etched by nital.

The extensometer will record the dimensional change of the specimen, and the transformation points can be obtained as shown in Fig.7.

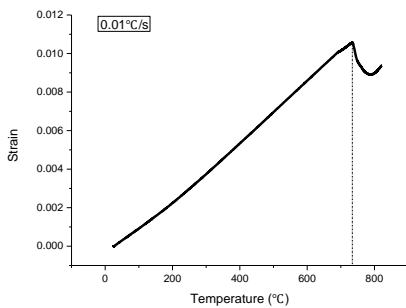


Fig.7 Thermal expansion curve (Heating rate: 0.01°C/s)

Then the A3 temperatures under different heating rates can be gotten from the expansion curve at the inflection point. Also the calculations are done with 1D model. The results are compared in Fig.8, it is easily found that the two results are almost close to each other and have the same increasing trend. It proves the validity of 1D model, also the 2D model.

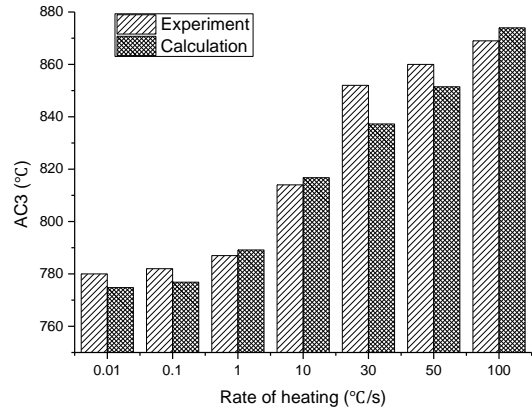


Fig.8 Comparison of A3 temperatures between experiment and calculation in 45 steel (Grain size: 20um)

SIMULATION OF AUSTENITE GRAIN GROWTH IN 2D MODEL

The 2D model calculation of austenite grain growth is performed using a 30 x 30-mesh with a parameter $a = 0.5$ um and a time step of 0.0006 s. The result of a simulation under a constant heating rate of 10°C/s is shown in Fig.9. The phase field in the microstructure is represented at four different times with different colors.

During the transformation process, it can be seen that the interface becomes a circle gradually. The corners of the grains become smooth, because diffusion occurs more rapidly in these regions.

Notice that when ferrite regions change to austenite progressively, some tips show up at the interface for some ferrite grains change to austenite faster than other grains. And the tips of the austenite regions become smooth gradually. The blue zones representing ferrite regions which are progressively dissolved in the austenitic matrix (red color).When the austenitization completes, the entire region become austenite region.

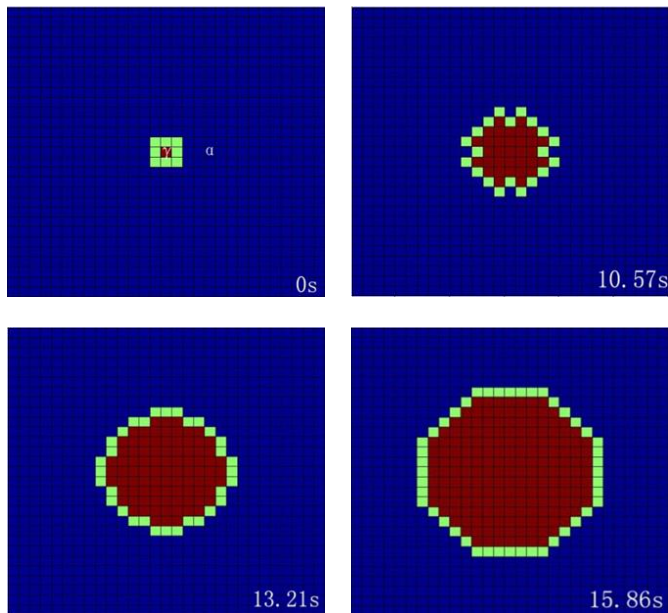


Fig.9 Evolution of microstructures during austenitization process (Grain size: 15 μ m)

DISCUSSION AND CONCLUSION

In the 2D model, the diffusion of carbon proceeds between central cell and neighboring cells, while there is no diffusion of carbon between central cell and corner cells. Therefore, some tips appear at these corner cells. If the model takes this factor into account, the interface will become smoother just like a circle. Because the model adopts the explicit finite volume technique, so its amount of computation is large. It will be faster using implicit finite volume technique.

It's effective to study the austenitizing process in hypoeutectoid Fe-C steels by a two-dimensional diffusion model based on Fe-C equilibrium phase diagram. The 2D model adopts a square grid and the results of 2D model agree with 1D model's corresponding results well. And as the heating rate or grain size increases, the difference between two models' final austenitization temperature decrease. Notice that when ferrite change to austenite progressively in 2D model (see Fig. 9), some tips show up at the interface for some ferrite grains change to austenite faster than other grains. And the tips of the austenite regions become smooth gradually. It is necessary to introduce curvature effects and homogenization of the carbon concentration if realistic morphologies and growth kinetics are to be simulated. Some essential experiments will be done to verify further the 2D model.

ACKNOWLEDGMENTS

This work was financially supported by the National Basic Research Program of China (973 Program) (No. 2011CB013404) and Project of National Science Foundation of China (51275254).

REFERENCES

- [1] Luo Qinghong, Li Chunzhi, ACTA METALLURGICA SINICA, 48(2012), 194-198
- [2] A. Jacot, M. Rappaz, Acta materialia 47 (1999) 1645-1651.
- [3] A. Jacot, M. Rappaz, Acta materialia 45 (1997) 575-585.
- [4] W. Kapturkiewicz, E. Fraś, A. A. Burbelko, Materials Science and Engineering: A 413 (2005) 352-357.
- [5] M. Umemoto, W. S. Owen, Metallurgical transactions 5 (1974) 2041-2046.
- [6] Q. Gao, Y. Liu, X. Di, L. Yu, Z. Yan, Z. Qiao, Nuclear Engineering and Design 256 (2013) 148-152.
- [7] F. L. G. D. Oliveira, M. S. Andrade, A. B. Cota, Materials Characterization 58 (2007) 256-261.
- [8] W. Zhang, J. W. Elmer, T. DebRoy, Scripta Materialia 46 (2002) 753-757.
- [9] M. Avrami, The Journal of Chemical Physics 7 (1939) 1103.
- [10] A. Jacot, M. Rappaz, R. C. Reed, Acta materialia 46 (1998) 3949-3962.
- [11] S. Lee, Y. Lee, Materials & Design 29 (2008) 1840-1844.
- [12] G. Y. Lai, W. E. Wood, R. A. Clark, V. F. Zackay, E. R. Parker, Metallurgical Transactions 5 (1974) 1663-167
- [13] Y. B. Guo, J. Sahni, International Journal of Machine Tools and Manufacture 44 (2004) 135-145.